Published August 1, 2016

In vivo determination of subcutaneous and abdominal adipose tissue depots in German Holstein dairy cattle[1]

C. Raschka,* L. Ruda,*[2] P. Wenning,* C.-I. von Stemm,† C. Pfarrer,‡ K. Huber,§ U. Meyer,‡ S. Dänicke,‡ and J. Rehage*

*Clinic for Cattle and †Institute for Anatomy, University of Veterinary Medicine Hannover, Foundation, Hannover, Germany; ‡Institute of Animal Nutrition, Friedrich-Loeffler-Institute (FLI), Federal Research Institute for Animal Health, Braunschweig, Germany; and §Institute of Animal Science, University of Hohenheim, Stuttgart, Germany

ABSTRACT: Ultrasonography was used as a noninvasive method for quantitative estimation of the subcutaneous and abdominal adipose tissue depots in dairy cattle. The prediction model was created and validated with a total of 29 German Holstein cows; 6 were in early lactation (≤100 d in milk [DIM]) and 16 were in advanced lactation (101 to 292 DIM). Seven cows were nonpregnant and nonlactating and had been off milk for 350 to 450 d. Transcutaneous assessment of the thickness of subcutaneous and retroperitoneal adipose tissue was done at 16 sites on the body surface of all cows. After completion of the ultrasonographic measurements, the cows were slaughtered and the adipose depots were separately weighed. A stepwise multivariate regression analysis of the ultrasonographic variables was performed to estimate the slaughter weights of the different fat depots. Slaughter weights of the fat depots ranged from 5.0 to 43.0 kg for subcutaneous adipose tissue (SCAT), from 13.7 to 98.8 kg for abdominal adipose tissue (AAT), from 3.4 to 30.3 kg for retroperitoneal adipose tissue (RPAT), from 5.2 to 39.6 kg for omental adipose tissue (OMAT), and from 4.0 to 35.8 kg for mesenteric adipose tissue (MAT). The relationship between calculated amount of fat and slaughter weight of fat had coefficients of determination (R^2) and root mean square errors (kg) of 0.88 and 3.4, respectively, for SCAT; 0.94 and 6.1, respectively, for AAT; 0.94 and 1.7, respectively, for RPAT; 0.83 and 3.2, respectively, for OMAT; and 0.95 and 1.6, respectively, for MAT. The accuracy of ultrasonographic measurement of the different fat depots appears sufficient for the quantitative assessment of internal and subcutaneous fat stores in cows. This method is noninvasive and therefore allows safe and repeated monitoring of the amount of stored fat in different adipose tissue depots of German Holsteins cows.

Key words: adipose tissue depots, dairy cows, noninvasive, quantitative estimation, ultrasonography

 J. Anim. Sci. 2016.94:2821–2834
doi:10.2527/jas2015-0103

INTRODUCTION

Mobilization of endogenous lipid stores normally occurs in early lactation when energy requirements exceed energy supply provided by voluntary feed intake. Poor adaptation to negative energy balance (**NEB**) with exceeding lipolysis can progress to lipid mobilization syndrome (**LMS**), which is still a major concern in modern dairy production (Drackley, 1999). Overconditioning of cows at calving is a major risk factor for LMS (Roche et al., 2009). Interestingly, overconditioned early-lactation cows with BCS of 4.0 or higher (Edmonson et al., 1989) had higher NEFA and β-hydroxybutyrate concentrations in plasma but a decrease in BCS that was similar to cows with average or below-average BCS (Rastani et al., 2001; Pires et al., 2013). This was thought to be attributable to mobilization of internal fat depots in addition to subcutaneous fat in cows

[1]The authors thank the Deutsche Forschungsgemeinschaft (DFG, Bonn, Germany) for financial support (RE 819/7-1). We gratefully acknowledge the staff of the Experimental Station of the Friedrich-Loeffler-Institute (FLI) in Brunswick for their excellent help in animal care and sample and data collection.

[2]Corresponding author: lenaruda@gmx.de

Received November 16, 2015.
Accepted May 3, 2016.

with NEB (Rastani et al., 2001; Pires et al., 2013). Regarding the accumulation of adipose tissue, the results of Drackley et al. (2014) pointed to the fact that BCS might lack sensitivity to detect visceral fat deposition. In humans and rodents, different adipose tissue depots react differently to metabolic stimuli (Yang and Smith, 2007), and studies in dairy cows suggest that subcutaneous and internal adipose tissue depots have different metabolic properties (Locher et al., 2011, 2012; Häussler et al., 2013; Saremi et al., 2014). Therefore, different adipose depots may play different roles in the pathogenesis of LMS. Because magnetic resonance imaging or computerized axial tomography (Shen et al., 2003) are impractical for imaging internal fat stores in cattle, BCS according to Edmonson et al. (1989) and ultrasonographic measurement of back fat thickness (**BFT**) are routinely used to assess body condition of dairy cows (Staufenbiel, 1992, 1997; Schröder and Staufenbiel, 2006; Hussein et al., 2013). Ultrasonography also was used to measure the thickness of the retroperitoneal adipose tissue layer (Kabara et al., 2014). Ultrasonographic measurements of the perirenal adipose tissue depot and rib fat provide good estimates of the slaughter weight of internal adipose depots of beef cattle (Ribeiro et al., 2008; Ribeiro and Tedeschi, 2012). In goats and sheep, ultrasonographic measurement of subcutaneous fat has been evaluated as a predictor of carcass composition and body fat partitioning (Teixeira et al., 2008; Ripoll et al., 2009; Peres et al., 2010). Ultrasonographic measurement of both muscle depth and perirenal adipose tissue effectively predicted abdominal fat depots in goats at different stages of gestation (Härter et al., 2014). A noninvasive method for repeated quantitative in vivo estimation of subcutaneous and abdominal adipose tissue depots and for differentiation of retroperitoneal, mesenteric, and omental fat would also be beneficial for monitoring internal fat depots and for studying the dynamics of adipose tissue changes in dairy cattle. The purpose of this study was, therefore, to develop an ultrasonography-based multiple regression model to predict the quantity of subcutaneous, abdominal, retroperitoneal, omental, and mesenteric fat stores in dairy cows.

MATERIALS AND METHODS

The trial was performed at the experimental station of the Institute of Animal Nutrition, Friedrich-Loeffler-Institute, Brunswick, Germany, and was approved by the Animal Welfare Council of the Lower Saxony State Office for Consumer Protection and Food Safety (**LAVES**), Oldenburg, Germany (reference number: 3392 452502-04-13/1102).

Animals and Study Design

For development and validation of an ultrasonography-based multiple regression model to predict the quantity of subcutaneous and abdominal fat stores, 24 pluriparous and 5 primiparous dairy cows were slaughtered to assess the amount of stored fat in the different depots. Cows were slaughtered because of management decisions of the farm's administration and 7 cows had been part of an experiment focusing on metabolism of overconditioned cows and, therefore, were overconditioned at slaughter (Locher et al., 2015). As a consequence, cows showed a broad range of body condition and were at different stages of production when slaughtered. Body weight at slaughter ranged from 547 to 867 kg (Table 1). Six cows were in early lactation (≤100 d in milk **[DIM]**) and 16 were in advanced lactation (101–292 DIM). The 7 cows taken from the research project were nonpregnant and nonlactating and were off milk between 350 and 450 d when they were slaughtered. The 29 cows were split into a study cohort ($n = 23$) for development of ultrasonography-based regression equations for the prediction of the quantity of fat stores and into a test cohort ($n = 6$) in which obtained regressions equations were tested.

Finally, the obtained regression model was applied to 12 multiparous transition cows (application cohort) at −42, 3, and 21 DIM. Details on management, feeding, and housing of these cows are given by Tienken et al. (2015a,b). Briefly, cows were housed in a free stall with cubicles and were fed with total mixed rations. Before parturition, the total mixed ration was based on 30% concentrate and 70% roughage, and after parturition, the dietary percentage of concentrate was gradually increased to 50% over 16 d. All diets were fed ad libitum.

Body Size Measurement

Body size was determined as described by Wildman et al. (1982) and Heinrichs et al. (1992) immediately before slaughter. For this purpose and for ultrasonography, cows were placed in a squeeze chute (Priefert Manufacturing, Mount Pleasant, TX). Sternum height, hook height, and withers height were measured to determine frame size. Hip width, heart girth, body length, and BW were also measured.

Ultrasonography

A Toshiba SSA-370A PowerVision 6000 ultrasound machine equipped with a 6 to 12 MHz (PLN-805AT) linear probe and a 2 to 7 MHz (PVM-375AT; all from Toshiba Medical Systems, Neuss, Germany) convex array transducer was used for transcutaneous ultrasonography. All sonographic images were obtained from the right side of the cows. The hair in the area to be examined

Table 1. Body weight; slaughter weight (mean ± SD and range) of subcutaneous adipose tissue (SCAT), total abdominal adipose tissue (AAT), retroperitoneal adipose tissue (RPAT), omental adipose tissue (OMAT), and mesenteric adipose tissue (MAT); and weight of fat depots relative to AAT in adult female German Holsteins in different production stages

Body weight and weight of fat depots (kg) in study cows in early lactation (≤100 DIM[1]; *n* = 6)						
Descriptive statistics	BW	SCAT	AAT	RPAT	OMAT	MAT
Mean	652	16.1	31.1	10.8	10.5	9.8
Range	616–701	6.91–28.0	17.2–59.0	4.74–20.6	6.50–17.3	6.0–21.1
SD	32.8	9.2	15.1	5.7	4.3	5.8
Body weight and weight of fat depots (kg) in study cows in advanced lactation (101–292 DIM; *n* = 16)						
	BW	SCAT	AAT	RPAT	OMAT	
Mean	664	13.9	31.0	9.09	12.4	
Range	547–765	5.0–30.0	13.7–56.7	3.36–21.8	5.20–31.3	
SD	64.2	7.9	13.1	4.8	5.0	
Body weight and weight of fat depots (kg) in nonpregnant, nonlactating study cows (*n* = 7)						
	BW	SCAT	AAT	RPAT	OMAT	MAT
Mean	795*	29.7*	81.4*	24.1*	29.5*	27.8*
Range	688–867	20.1–43.0	65.8–98.8	19.7–30.3	19.3–39.6	22.6–35.8
SD	81.5	8.5	14.1	3.5	7.0	5.6
Ratio of fat depots to AAT in study cows in early lactation (≤100 DIM; *n* = 6)						
	SCAT:AAT	RPAT:AAT	OMAT:AAT	MAT:AAT		
Mean	0.51[a]	0.34[a]	0.35[a]	0.31		
Range	0.38–0.83	0.28–0.43	0.30–0.39	0.24–0.36		
SD	0.16	0.05	0.04	0.05		
Ratio of fat depots to AAT in study cows in early lactation (101–292 DIM; *n* = 16)						
	SCAT:AAT	RPAT:AAT	OMAT:AAT	MAT:AAT		
Mean	0.43[ab]	0.29[b]	0.40[b]	0.31		
Range	0.27–0.58	0.23–0.39	0.36–0.47	0.24–0.38		
SD	0.10	0.07	0.03	0.04		
Ratio of fat depots to AAT in nonpregnant, nonlactating study cows (*n* = 7)						
	SCAT:AAT	RPAT:AAT	OMAT:AAT	MAT:AAT		
Mean	0.36[b]	0.30[b]	0.36[a]	0.34		
Range	0.26–0.43	0.26–0.4	0.30–0.40	0.28–0.38		
SD	0.07	0.03	0.04	0.03		

[a,b]Means with different superscripts indicate significant difference ($P < 0.05$) between production stages in corresponding depots.

[1]DIM = d in milk.

*Means significantly different from corresponding means in early lactating and advanced lactating cows ($P < 0.05$).

was clipped, and conductive gel was applied to improve the bond between the skin and the transducer. To avoid bias caused by compression of the tissue during ultrasonography, no additional manual pressure was applied to the transducer. The thickness of tissues was measured on frozen images using the electronic calipers. The anatomic measurement sites and directions of ultrasound beam are described in Table 2 and depicted in Fig. 1 through 6. The thickness of the fat surrounding the kidney was determined as described (Ribeiro et al., 2008) with the modification of an additional measurement in a dorsoventral direction. Back fat thickness was measured in the sacrotuberal region according to Staufenbiel (1992). However, in the present study, hair was clipped at the examination site. To determine the accuracy of the ultrasonographic measurements, the CV (%) and the SD were calculated using 2 cows that did not belong to the

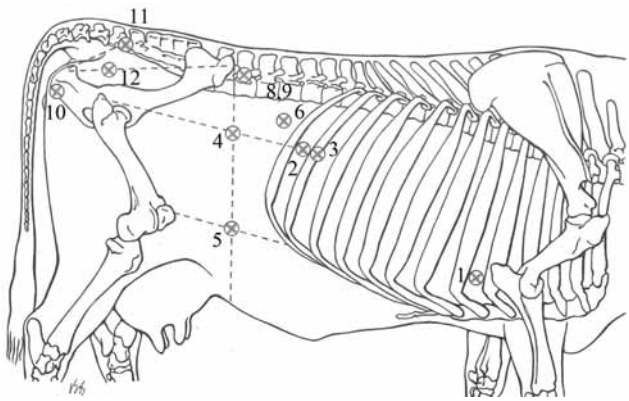

Figure 1. Schematic illustration of the anatomic locations used for the ultrasonographic measurements of tissue layers in German Holstein cows; see Table 2.

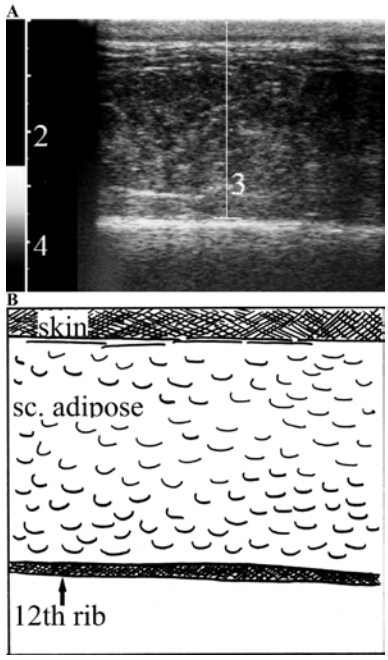

Figure 2. (A) Ultrasonogram (SSA 370A Toshiba Version K PowerVision 6000 and 6 MHz linear probe; Toshiba Medical System, Neuss, Germany) of the subcutaneous fat layer over the 12th rib (position 3). (B) Schematic drawing of sonogram 2A. sc. = subcutaneous

29-cow study group. Serial ultrasonographic measurements were made 5 times at each measurement site on 2 consecutive days in both cows, generating 4 CV for each measurement site. The mean CV and SD were then calculated for each measurement site

Slaughter

All cows were slaughtered, and omental adipose tissue (**OMAT**), retroperitoneal adipose tissue including adipose tissue surrounding the kidney (**RPAT**), adipose tissue stored in the mesentery including adipose tissue in the pelvic cavity (mesenteric adipose tissue; **MAT**), and subcutaneous adipose tissue (**SCAT**) were removed from the carcass and weighed separately. The total abdominal adipose tissue (**AAT**) was calculated as the sum of OMAT, MAT, and RPAT.

Statistical Analysis

All data were statistically evaluated using SAS 9.3 (SAS Inst. Inc., Cary, NC). In slaughtered cows, the ratio of actual slaughter weights of SCAT and AAT (SCAT:AAT) and the ratios of the 3 abdominal compartments to AAT (OMAT:AAT, RPAT:AAT, and MAT:AAT) were calculated. For data that were normally distributed (Proc Univariate), absolute weights and calculated ratios were subjected to a 1-way ANOVA (Proc GLM) with the factor production stage. When the group effect was significant ($P < 0.05$), a subsequent

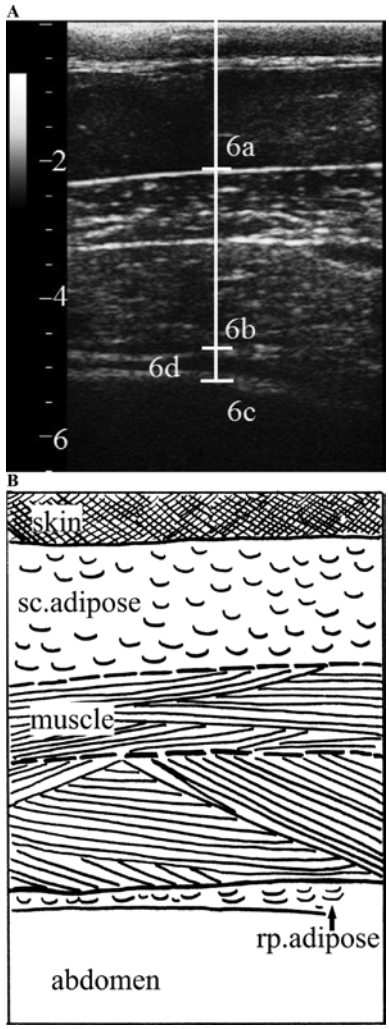

Figure 3. (A) Ultrasonogram (SSA 370A Toshiba Version K PowerVision 6000 and 6 MHz linear probe; Toshiba Medical System, Neuss, Germany) of the abdominal wall in the right paralumbar fossa (position 6a–6d). 6a: Subcutaneous fat layer from skin to the deep fascia; 6b: distance between skin and muscle margin away from the transducer; 6c: distance between skin and peritoneum; and 6d: distance 6c minus 6b representing retroperitoneal fat layer. Analogous distances were measured at locations 4 and 5. (B) Schematic drawing of sonogram 3A. sc. = subcutaneous; rp. = retroperitoneal.

Ryan–Einot–Gabriel–Welsch multiple range test was used to test for differences between groups.

For selection of 6 test cows from the 29 slaughter cows, the range of adipose mass in fat depots weighed at slaughter in all animals ($n = 29$) was divided into 6 equal quantiles. Out of each quantile, the last individual was chosen for validation of the model and was, therefore, removed from the study group.

Ultrasonographic measurements in all animals had been done in duplicate and the mean was used for analysis. A stepwise multivariate linear regression analysis (Proc Reg) of the ultrasonographic and body size variables was accomplished with the data obtained in the 23 cows remaining in the study group to determine the slaughter weights (in kg) of the different fat depots. Entry level and stay level were set to $P = 0.05$.

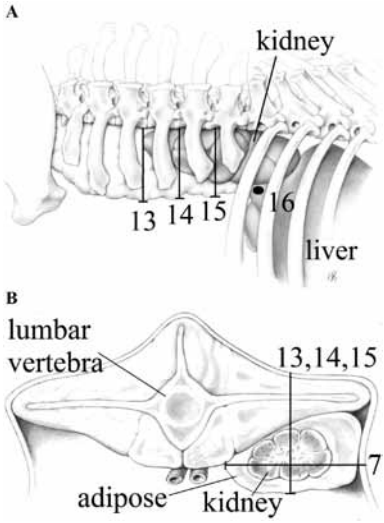

Figure 4. Illustration of the vertical (A: KD1; position 13, KD2; position 14, KD3; position 15) and horizontal transcutaneous ultrasonographic (B: KL; position 7) measurements of tissue layers in the kidney region and at the dorsal margin of the liver (A: ICL; position 16). KD1 = measurement in the intertransverse space where the caudal pole of the kidney is visible in dorsoventral direction; KD2 = measurement in the intertransverse space directly cranial to KD1 in dorsoventral direction; KD3 = measurement in the intertransverse space directly cranial to KD2 in dorsoventral direction; KL = measurement in the flank directly below the lumbar transverse processes over the kindney in a horizontal direction; ICL = measurements in the 12 intercostal space at the level of the dorsal liver margin.

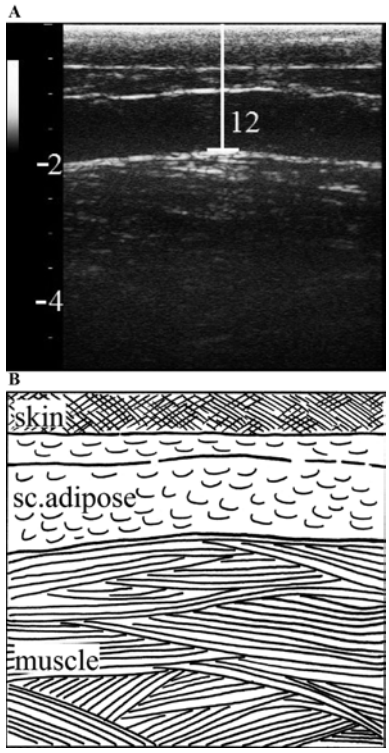

Figure 5. (A) Ultrasonogram (SSA 370A Toshiba Version K PowerVision 6000 and 6 MHz linear probe; Toshiba Medical System, Neuss, Germany) of the subcutaneous fat layer according to Schröder and Staufenbiel (2006; position 12). (B) Schematic drawing of sonogram 5A. sc. = subcutaneous.

Regressions for prediction of SCAT, AAT, OMAT, MAT, and RPAT were calculated. The coefficients of determination (R^2) and root mean square errors (**RMSE**; in kg) were calculated to assess the accuracy of the equations.

A linear regression between actual weight of adipose mass weighed at slaughter and the respective adipose mass predicted by the model was performed with the 6 test cows taken out of the group of slaughtered cows before multiple regression analysis. Deviations in kilograms between actual slaughter weight and predicted weight were depicted using Bland–Altman plots.

Results on quantitative assessment of different fat depots obtained in the 12 transition cows from the application group by means of the developed regression models were normally distributed and analyzed using a 1-way ANOVA for repeated measurements (Proc GLM) with the factor time. When the time effect in the model was significant ($P < 0.05$), paired tests were used to assess differences between production stages.

RESULTS

Slaughter and Body Size Parameters

Actual slaughter weights and ratios of the different fat depots are shown in Table 2. In general, the actual slaughter weight of AAT varied between approximately 3 times to twice that of the SCAT, and the OMAT, RPAT, and MAT accounted for approximately one-third each of AAT. The cow with the highest body condition had 8 times more SCAT, 7 times more AAT, 9 times more RPAT, 8 times more OMAT, and 9 times more MAT than the cow with the lowest body condition. Absolute amounts of SCAT, AAT, RPAT, OMAT, and MAT as well as BW did not differ between lactating cows, but nonpregnant, nonlactating cows had higher amounts of adipose in all depots. The SCAT:AAT ratio was higher in cows in early lactation than in cows that were nonpregnant and nonlactating. The OMAT:AAT ratio was higher in advanced lactation cows than in cows in early lactation and nonlactating cows. In contrast, the RPAT:AAT ratio was highest in early lactating cows and significantly different from advanced lactating and nonlactating cows. The ratio of MAT to AAT did not differ between groups.

Linear correlations between adipose tissue depots in all slaughtered cows ($n = 29$) are shown in Table 3. There were strong correlations between AAT and its 3 components (OMAT, MAT, and RPAT; $r = 0.95$ to 0.97, $P < 0.001$) and between SCAT and AAT ($r = 0.89$, $P < 0.001$; Table 3). Between RPAT, OMAT, and MAT, correlations ranged from 0.84 (OMAT vs. MAT; $P < 0.001$) to 0.92 (RPAT vs. OMAT; $P < 0.001$). When grouped according to the production stage, these correlations remained almost unchanged in early and advanced

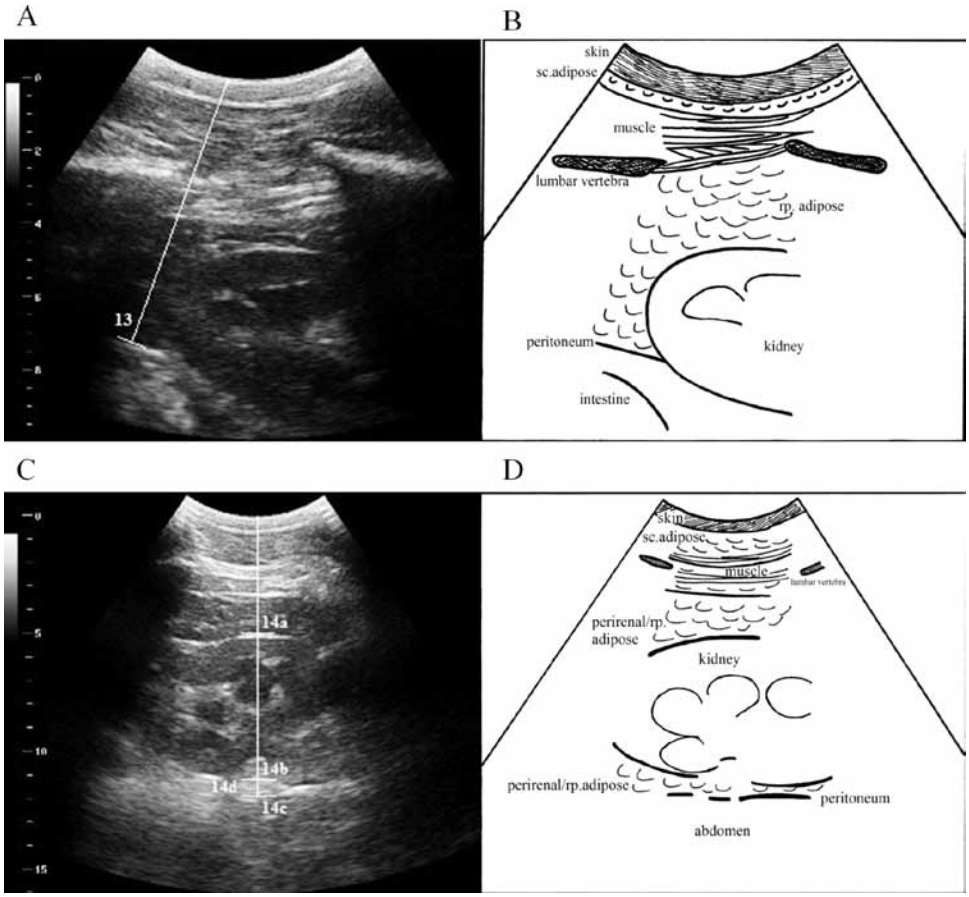

Figure 6. (A) Ultrasonography in a vertical direction at the lumbar intertransverse space where the caudal pole of the kidney was visible (position 13); distance between skin and peritoneum was measured. (B) Schematic drawing of ultrasonogram A . (C) Ultrasonography in a vertical direction 1 lumbar transverse space cranial to the position shown in A (position 14). 14a: Distance between skin and kidney; 14b: distance between skin and ventral kidney margin; 14c: distance between skin and peritoneum; and 14d: difference between distances 14c and 14b representing the thickness of the ventral layer of the perirenal fat. Analogous distances were measured at location 15. (C) Schematic drawing of sonogram C; sc. = subcutaneous; rp. = retroperitoneal ; ultrasonography performed with SSA 370A Toshiba Version K PowerVision 6000 and 3 MHz convex array transducer; Toshiba Medical System, Neuss, Germany)

stages of lactation as well as in nonpregnant and nonlactating cows and ranged from $r = 0.79$ to $r = 0.98$ (data not shown). Body size parameters are shown in Table 4.

Ultrasonography

Calculated CV of sonographic measurements were below 5% except for the distances between the muscle margin and the peritoneum at the abdominal wall (**AW1d**; 18.1 ± 6.5%; **AW2d**; 17.9 ± 12.5 and **AW3d**; 23.9 ± 7.9%), as well as the distances between the distal kidney margins and the peritoneum (**KD2d**; 20.1 ± 5.4%; **KD3d**; 17.7 ± 6.4), and the distance between the thoracic muscles and the liver (**ICLc**; 12.5 ± 12.5%; Table 5). Results of ultrasonographic measurements in slaughtered cows are presented in Table 6.

Development of Regression Models for Quantitative Assessment of Fat Depots in Study Cows

Regression equations for estimating weights of fat depots in are shown in Tables 7 (SCAT) and 8 (AAT, OMAT, RPAT, and MAT). The thickness of the subcutaneous fat layer over the 12th rib (**R12**) and the thickness of the abdominal wall (**AW3c**) were selected in the model for estimating the amount of SCAT with R^2 of 0.89 and RMSE of 3.67 kg. From the 35 sonographic variables and 7 body size and constitution parameters that were evaluated, 7 sonographic variables were finally selected by multivariate regression analysis for assessment of AAT and its components OMAT, RPAT, and MAT. The prediction equations for RPAT and OMAT included 2 sonographic variables; R^2 and RMSE were 0.94 and 1.73, respectively, for RPAT, and 0.84 and 3.18, respectively, for OMAT (Table 8). Four sonographic variables were selected for calculation of MAT; the respective R^2 and RMSE were 0.94 and 1.58. For AAT, 3 sonographic variables were selected, resulting in R^2 and RMSE of 0.94 and 6.14 (Table 8).

Validation of the Model in Test Cows

Linear regression of actual slaughter weights with the predicted weights in the 6 test cows led to determination

Table 2. Anatomic locations for ultrasonographic measurements and directions of ultrasound beam

Nr.	Anatomic location	Description of location and direction of ultrasound beam	Measured distance	Relevant figures
1	ICO	Fifth intercostal space immediately caudal to olecranon		1
2	IC12	12th intercostal space at the level of the greater trochanter		1
3	R12	12th rib (at the level of the greater trochanter)		1 and 2
4	AW1 (a–d)	Point of interception of a vertical line through the last lumbar vertebra and a horizontal line through the greater trochanter	a: subcutaneous fat; b: skin to muscle margin away from transducer; c: skin to peritoneum; and d: muscle margin away from transducer to peritoneum	1
5	AW2 (a–d)	Point of interception of a vertical line through the last lumbar vertebra and a horizontal line through the patella	a: subcutaneous fat; b: skin to muscle margin away from transducer; c: skin to peritoneum; and d: muscle margin away from transducer to peritoneum	1
6	AW3 (a–d)	Center of paralumbar fossa	a: subcutaneous fat; b: skin to muscle margin away from transducer; c: skin to peritoneum; and d: muscle margin away from transducer to peritoneum	1 and 3
7	KL	In the flank below the lumbar transverse processes over the kidney in a horizontal direction (Ribeiro et al., 2008)		4
8	TP2	In the middle between the tips of the transverse and spinous processes of the last lumbar vertebra in a ventral longitudinal direction		1
9	TP3	Lateral third of the distance between the tips of the transverse and spinous processes of the last lumbar vertebra in a ventral longitudinal direction		1
10	IT	Ischial tuberosity		1
11	BT	Base of the tail		1
12	BFT	Back fat thickness (according to Staufenbiel [1992])		1 and 5
13	KD1	Lumbar intertransverse space where caudal pole of kidney is visible, measuring from skin to peritoneum		4 and 6
14	KD2 (a–d)	Intertransverse space cranial to KD1	a: skin to kidney; b: skin to kidney margin away from transducer; c: skin to peritoneum; and d: fat capsule between b and c	4 and 7
15	KD3 (a–d)	Intertransverse space cranial to KD2	a: skin to kidney; b: skin to kidney margin away from transducer; c: skin to peritoneum; and d: fat capsule between b and c	4
16	ICL (a–c)	12th intercostal space at dorsal liver margin	a: skin to muscle margin away from transducer; b: skin to liver; and c: fat between liver and musculature	4

coefficients of R^2 = 0.84 to 0.96. The linear regressions between actual slaughter weights and predicted weights of the different depots as well as the respective Bland–Altman plots are shown in Fig. 7 and 8.

Table 3. Pearson's correlation between slaughter weights of subcutaneous adipose tissue (SCAT), retroperitoneal adipose tissue (RPAT), omental adipose tissue (OMAT), mesenteric adipose tissue (MAT), and total abdominal adipose tissue (AAT) in 29 German Holsteins

Depot	SCAT	AAT	RPAT	OMAT
AAT	0.89			
P-value	<0.001			
RPAT	0.87	0.97		
P-value	<0.001	<0.001		
OMAT	0.79	0.95	0.92	
P-value	<0.001	<0.001	<0.001	
MAT	0.90	0.96	0.90	0.84
P-value	<0.001	<0.001	<0.001	<0.001

Application of the Model to Transition Cows

The predicted weights of the different fat depots for transition cows repeatedly measured from −42 until 21 DIM are given in Table 9. The total abdominal fat depot AAT and its subdivisions RPAT, MAT, and OMAT increased from −42 until 3 DIM and then decreased until 21 DIM (P < 0.05–0.001). In contrast, SCAT did not

Table 4. Sternum height (SH), hook height (HH), height at the withers (WH), hip width (HW), heart girth (HG), body length (BL), and BW in 29 German Holsteins (assessment according to Wildman et al., 1982)

Body size parameter	Mean	Range
SH, cm	66	54–73
HH, cm	150	139–161
WH, cm	150	139–159
HW, cm	57	50–67
HG, cm	217	197–241
BL, cm	179	166–189
BW, kg	693	547–867

Table 5. Ultrasonographic measurements (mean, CV, and mean CV [SD]) in 2 German Holstein cows

		Mean, mm	CV, %	Mean, mm	CV, %	Mean, mm	CV, %	Mean, mm	CV, %	Mean CV,
Nr.	Variable[1]	Cow 1, Day 1		Cow 1, Day 2		Cow 2, Day 1		Cow 2, Day 2		% (SD)
1	ICO	5.7	2.5	5.2	2.4	6.4	3.4	6.1	1.4	2.4 (0.8)
2	IC12	17.9	1.3	18.9	1.5	5.6	0.5	5.9	4.1	1.9 (1.6)
3	R12	18.0	0.3	18.0	2.8	5.8	0.6	5.7	1.4	1.3 (1.3)
4	AW1a	4.6	4.0	5.6	1.9	7.1	4.5	7.2	2.6	3.3 (1.2)
	AW1b	22.4	1.5	22.4	2.8	19.8	1.3	19.9	2.7	2.1 (0.8)
	AW1c	23.9	1.4	24.1	1.6	21.1	1.5	21.3	3.8	2.1 (1.2)
	AW1d	1.4	9.3	1.7	21.7	1.3	17.	1.42	24.1	18.1 (6.5)
5	AW2a	6.3	4.1	6.5	3.8	6.4	4.2	6.1	7.5	4.9 (1.8)
	AW2b	24.7	2.8	25.6	3.4	25.7	3.3	24.6	3.1	3.2 (0.3)
	AW2c	26.2	2.6	27.1	3.6	27.3	3.2	25.8	1.8	2.8 (0.8)
	AW2d	1.5	8.6	1.5	12.4	1.5	14.2	1.2	36.3	17.9 (12.5)
6	AW3a	13.2	2.7	12.9	0.5	8.8	1.7	9.6	4.5	2.4 (1.7)
	AW3b	25.6	1.3	26.5	2.9	19.1	3.5	20.5	2.2	2.5 (1.0)
	AW3c	26.7	0.4	27.7	2.5	20.3	4.5	21.5	1.9	2.4 (1.7)
	AW3d	1.2	21.9	1.1	26.1	1.2	33.	1.1	14.3	23.9 (7.9)
7	KL	99.8	0.1	101.1	1.2	81.4	0.8	82.6	2.4	1.1 (1.0)
8	TP2	10.2	2.4	10.4	1.8	7.6	2.7	7.2	6.1	3.3 (2.0)
9	TP3	10.9	1.1	10.1	3.58	7.7	0.8	7.2	3.3	2.2 (1.4)
10	IT	10.3	1.2	11.2	5.0	8.3	3.6	7.2	3.0	3.2 (1.6)
11	BT	13.1	1.8	12.5	3.0	6.9	1.5	6.8	2.3	2.2 (0.7)
12	BFT	18.0	0.3	18.2	2.5	6.8	2.0	6.5	2.1	1.7 (1.0)
13	KD1	121.2	0.4	119.8	1.3	99.9	0.7	101.2	1.7	1.0 (0.6)
14	KD2a	76.3	2.3	66.0	1.0	53.8	1.6	53.4	3.0	2.0 (0.9)
	KD2b	114.8	0.7	116.8	2.0	101.6	1.1	102.0	1.7	1.4 (0.6)
	KD2c	121.4	1.7	126.2	1.0	112.2	0.3	110.0	0.6	0.9 (0.6)
	KD2d	6.6	23.0	9.4	23.7	10.6	12.1	8.0	21.7	20.1 (5.4)
15	KD3a	79.8	2.3	84.5	4.5	56.1	1.4	55.8	3.4	2.9 (1.3)
	KD3b	117.8	1.1	115.2	2.8	110.6	1.4	108.2	2.3	1.9 (0.8)
	KD3c	122.8	0.7	125.6	1.1	121.2	0.7	119.8	1.6	1.0 (0.4)
	KD3d	5.0	20.0	10.4	25.5	10.6	11.0	11.6	14.4	17.7 (6.4)
16	ICLa	31.5	0.3	36.0	3.2	19.8	3.6	20.0	3.1	2.6 (1.6)
	ICLb	35.7	0.6	39.5	3.3	23.9	2.5	23.8	1.37	1.9 (1.1)
	ICLc	4.2	6.5	3.5	9.0	4.12	22.1	3.8	12.5	12.5 (12.5)

[1]See Table 1.

show a significant increase between −42 and 3 DIM but decreased between 3 and 21 DIM ($P < 0.01$).

DISCUSSION

Changes in Proportional Shares and Correlations between Slaughter Weight of Adipose Depots

In this study, cows in different stages of lactation and also clearly overconditioned, nonlactating cows from a previous study (Locher et al., 2015) were used to ensure that cows with a wide range in body condition (Table 1) were available for the development of the regression equations for assessment of quantities of different fat depots. In the nonlactating, nonpregnant cows, the SCAT:AAT ratio was significantly lower than in early lactating cows. Also, the RPAT:AAT ratio was lower in cows in advanced stages of lactation and the nonlactating cows compared with cows in early lactation. These results may indicate asynchronicity in storage in and mobilization of fat from different adipose tissues in dairy cows in periods of positive or negative energy balance, respectively. The observation is in accordance with results reported by Drackley et al. (2014), who found a relatively higher accumulation of fat into internal stores within a fattening period of 8 wk in cows on a high-energy diet in comparison with their counterparts fed a lower-energy diet, even though the amount of subcutaneously stored fat did not appear to differ. The lack of sensitivity in BCS to detect visceral fat deposition as reported by Drackley et al. (2014) might be of particular importance in overconditioned cows.

Also, the studies by von Soosten et al. (2011) and Locher et al. (2011) already suggested that more abdominal fat than subcutaneous fat is mobilized when NEB occurs. However, by measuring BFT (Staufenbiel, 1992,

Table 6. Subcutaneous and retroperitoneal tissue layer thickness (mean and range) determined via transcutaneous ultrasonography at defined anatomic locations in 29 German Holstein cows

Nr.	Variable[1]	Mean, mm	Range, mm
1	ICO	6.2	4–11
2	IC12	15.1	5–30
3	R12	20.7	7–35
4	AW1a	7.6	4–18
	AW1b	26.7	12–52
	AW1c	28.6	13–55
	AW1d	1.9	1–4
5	AW2a	8.2	5–18
	AW2b	34.4	20–63
	AW2c	36.5	21–66
	AW2d	2.1	1–6
6	AW3a	12.4	4–23
	AW3b	29.5	13–67
	AW3c	31.4	14–69
	AW3d	1.9	1–4
7	KL	113.8	88–140
8	TP2	10.8	4–23
9	TP3	11.0	4–24
10	IT	13.3	7–34
11	BT	13.4	4–41
12	BFT	12.3	4–25
13	KD1	108.6	54–209
14	KD2a	70.2	31–139
	KD2b	137.3	68–211
	KD2c	151.0	99–219
	KD2d	13.7	8–23
15	KD3a	70.8	26–119
	KD3b	144.9	87–199
	KD3c	158.8	101–213
	KD3d	14.0	8–23
16	ICLa	31.4	14–69
	ICLb	37.5	16–80
	ICLc	5.7	3–10

[1]See Table 1.

1997) and the thickness of retroperitoneal fat according to Kabara et al. (2014), it is not possible to compare the relative contribution of different depots to fat mobilization during the transition period and early lactation. The method described in the present study allows the estimation of the amount of fat stored in various depots and thereby facilitates comparison among depots.

Estimating Subcutaneous Adipose Tissue

In the present study, the best predictors for the total amount of SCAT were the thickness of the subcutaneous fat layer at R12 (Fig. 1, position 3; Table 2) and the thickness of the abdominal wall in the dorsal region of the right flank (Fig. 1, position 6; Table 2, AW3c). Measurement of the subcutaneous fat layer in the region of the R12 also has been used and validated for the assessment of body composition and expected carcass quality in beef cattle (Lancaster et al., 2008, 2009). Back fat thickness in the sacrotuberal region is measured to estimate body condition in dairy cows (Staufenbiel, 1992). In contrast, multiple stepwise regression analysis herein found the thickness of the subcutaneous fat layer over the R12 (Table 2), rather than BFT, to be one of the most reliable determinants of the amount of SCAT in the present study. This supports findings of Schröder and Staufenbiel (2006), who also found the subcutaneous fat layer at R12 reflects the total amount of SCAT more precisely than BFT. Nevertheless, those authors favored the sacral area for measuring BFT in dairy cows because of a high correlation with total body fat (r = 0.9) and to facilitate comparison of BFT and BCS. The thickness of the subcutaneous fat at R12 is a valuable predictor not only for SCAT but also for AAT and its component RPAT (Table 8). This might mean that the thoracolumbar region may be a more precise indicator of body condition than the sacrotuberal area.

Table 7. Multivariate linear regression analysis of subcutaneous adipose tissue (SCAT) and ultrasonographic measurements of tissue layers and body size parameters in 23 German Holstein cows

Statistical parameter	SCAT		
P-value	<0.001		
R^2	0.88		
RMSE[1]	3.4		
Variable[2]	Parameter estimate	SE	*P*-value
Intercept	−6.66	1.98	0.003
R12	0.72	0.15	<0.001
AW3c	0.31	0.10	0.061

[1]RMSE = root mean square error.

[2]R12 = subcutaneous fat over the 12th rib at the level of the greater trochanter; AW3c = the thickness of the abdominal wall at the center of the paralumbar fossa.

Estimating Abdominal Adipose Tissue and Its Components

To obtain the most accurate estimate of MAT and OMAT, we attempted to identify anatomic sites for direct ultrasonographic assessment of adipose depots in the abdominal cavity. Various sites in both flanks were tested, but gas-filled intestines and marked organ movement related to breathing and gastrointestinal motility made it impossible to accurately identify and measure the tissues of interest. Therefore, measurement of abdominal fat was limited to the retroperitoneal fat. Repeated measurements measuring the fat layer directly adjacent to the peritoneum at all sites (AW1d, AW2d, AW3d, KD2d, and KD3d; Table 2) had mean CV of more than 5%

Table 8. Multivariate linear stepwise regression analysis of total abdominal adipose tissue (AAT), retroperitoneal adipose tissue (RPAT), omental adipose tissue (OMAT), mesenteric adipose tissue (MAT) and ultrasonographic measurements of tissue layers and body size parameters in 23 German Holstein cows

Statistical parameter	AAT			RPAT			OMAT			MAT		
P-value	<0.001			<0.001			<0.001			<0.001		
R^2	0.94			0.94			0.84			0.94		
RMSE[1]	6.1			1.7			3.2			1.6		
Variable[2]	Parameter estimate	SE	*P*-value	Parameter estimate	SE	*P*-value	Parameter estimate	SE	*P*-value	Parameter estimate	SE	*P*-value
Intercept	−39.5	5.65	<0.001	−9.55	1.61	<0.001	−2.32	1.70	0.19	−12.8	1.92	<0.001
R12	1.02	0.26	0.001	0.62	0.05	<0.001						
BFT							0.55	0.20	0.013			
AW1b	0.92	0.22	<0.001							0.38	0.09	<0.001
AW3b							0.37	0.09	<0.001	1.73	0.64	0.015
AW3c										−1.45	0.62	0.031
KD2c	0.25	0.05	<0.001							0.07	0.02	<0.001
KD3b				0.06	0.01	<0.001						

[1]RMSE = root mean square error.

[2]R12 = subcutaneous fat over the 12th rib; BFT = back fat thickness; AW1b = the distance from the skin to the distal muscle margin above the peritoneum at the point of interception of a vertical line trough the last lumbar vertebra and a horizontal line trough the patella; AW3b = the distance from the skin to the distal muscle margin above the peritoneum at the center of the paralumbar fossa; AW3c = the thickness of the abdominal wall at the center of the paralumbar fossa; KD2c = the distance from the skin to the peritoneum in the intertransverse space directly cranial to intertransverse space where the caudal pole of the kidney is visible; KD3b = the distance from the skin to the distal kidney margin in the intertransverse space directly cranial to KD2.

(Table 5), and none of these sites was selected in the model for equations predicting fat depots (Tables 7 and 8). Nevertheless, multiple regression analysis generated equations that indirectly determined MAT and OMAT using fat measurements in the abdominal wall and kidney region (Tables 2 and 8). Similarly, the amount of omental fat in goats could be predicted from the measured amount of kidney fat and BW using a multiple regression model (Härter et al., 2014). The measurements selected by the stepwise regression analysis to estimate the amount of AAT and its components included layers of the long back muscles or the abdominal muscles, and therefore, the measurements were affected by the amount of intra- and intermuscular fat. We did not measure the thickness of intermuscular fat layers or intramuscular fat by means of ultrasound-based texture analysis (Kim et al., 1998), which may have provided more precise information than merely measuring the thickness of tissue layers. However, the percentage of inter- and intramuscular fat was not identified as one of the best predictors for the mass of total physically separable internal body fat—a depot comparable with the AAT measured in the present study—in beef cattle of different breeds, sex, and age (Ribeiro and Tedeschi, 2012).

Effects of Body Size

In sheep and goats, BW is an important predictor of the amount of abdominal and subcutaneous fat stores (Teixeira et al., 2008; Ripoll et al., 2009; Peres et al., 2010; Härter et al., 2014) and it appears logical to assume that the same is true in cattle. However, all body size parameters were eliminated from our model and, therefore, were not used for the quantitative estimation of the different adipose tissue depots. It should be remembered that German Holstein cows of similar

Table 9. Predicted weight of fat depots as estimated by an ultrasonographic-based multiple regression model in German Holstein cows (n = 12) from −42 until 21 d in milk (DIM)

	Predicted weight of fat depots (kg) of application cohort[1]														
	SCAT			AAT			RPAT			OMAT			MAT		
Descriptive	DIM														
parameter	−42	3	21	−42	3	21	−42	3	21	−42	3	21	−42	3	21
Mean	15.6[a]	18.0[a]	12.5[b]	37.7[a]	50.6[b]	30.8[c]	4.3[a]	7.1[b]	2.1[c]	11.7[a]	14.8[b]	12.3[a]	10.8[a]	14.8[b]	8.8[c]
SD	3.6	5.7	4.0	10.0	12.7	9.3	2.6	2.9	2.7	2.4	4.9	4.3	2.6	3.9	3.1

[a–c]Means with different superscripts within 1 depot significantly differ ($P < 0.05$).

[1]SCAT = subcutaneous adipose tissue; AAT = abdominal adipose tissue; RPAT = retroperitoneal adipose tissue; OMAT = omental adipose tissue; MAT = mesenteric adipose tissue.

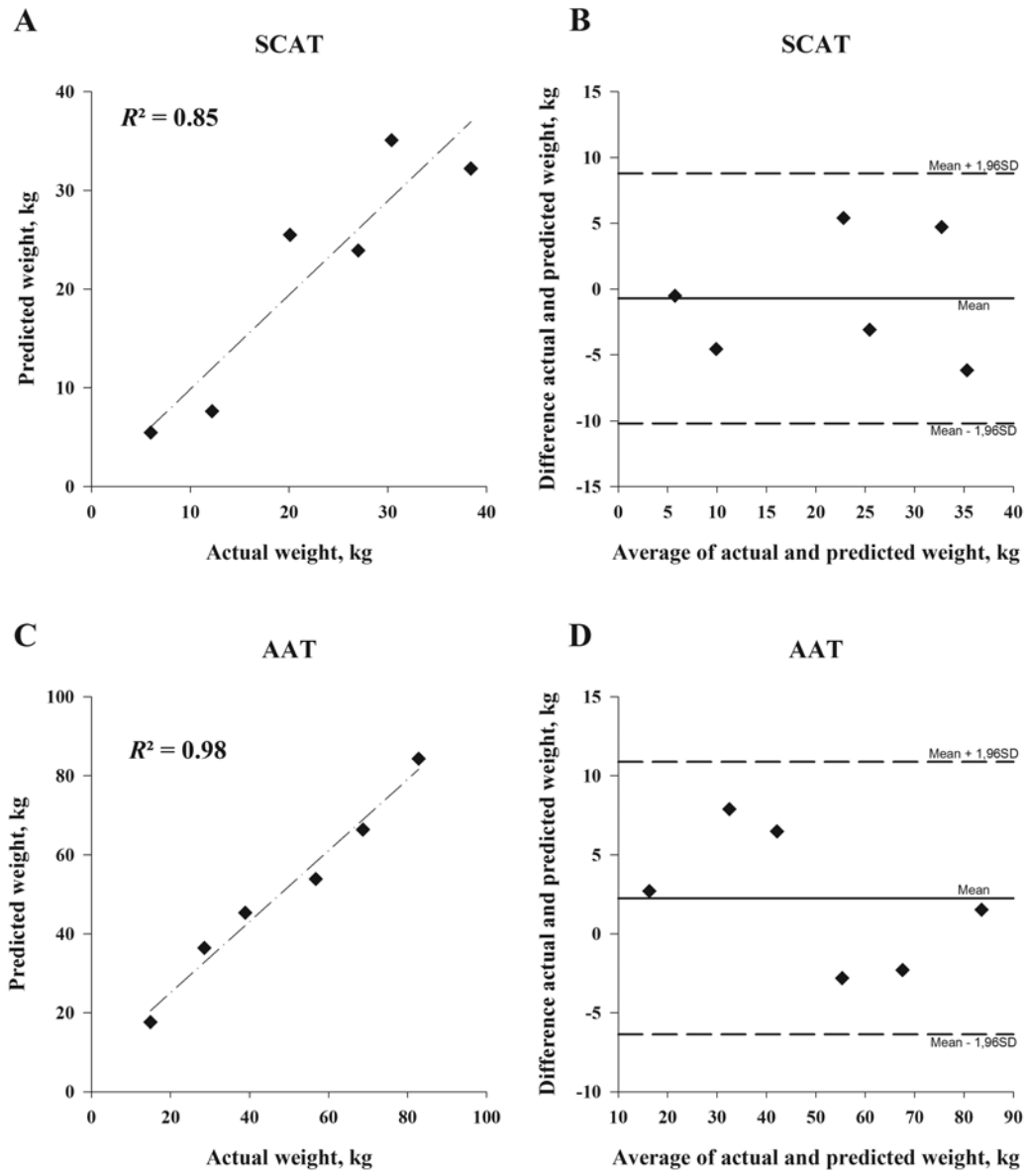

Figure 7. (A,C,) Linear regression between the actual slaughter weight of an adipose tissue depot and its weight predicted by a multivariate linear regression model based on ultrasonographic measurements of fat layers in 6 test German Holsteins cows. (B,D,) Bland–Altman plot of the difference between over the average of predicted and actual slaughter weights. SCAT = subcutaneous adipose tissue; AAT = abdominal adipose tissue

size were used in the present study and that a lack of difference in body size parameters may have contributed to their elimination from the model.

Applicability

Judging by the coefficients of determination (Tables 7 and 8), ultrasonographic estimation of AAT and its components appears slightly more precise than that of SCAT, even though ultrasonographic measurements directly reflected the SCAT depot whereas OMAT and MAT were indirectly calculated from proxy measurements. It is possible that these findings were affected by the slaughter protocol. The carcass was manually skinned with a butcher knife, and a certain portion of SCAT was removed with the hide. Likewise, a certain bias may have occurred when the RPAT was removed, because some of the retroperitoneal fat may have been left on the carcass because of broad attachment to the musculature and ribs. In relative terms, the portion of fat remaining on the hide or attached to the musculature and ribs is larger in thin animals than in fat animals. Therefore, our calculations may be less accurate when applied to lean cows with a small amount of body fat. In contrast, all components of the OMAT and the MAT are more easily removed from the gastrointestinal tract and the carcass, and therefore, the amount of fat not removed from these areas was smaller. These circumstances provide a possible explanation for the lower coefficients of determination associated with the

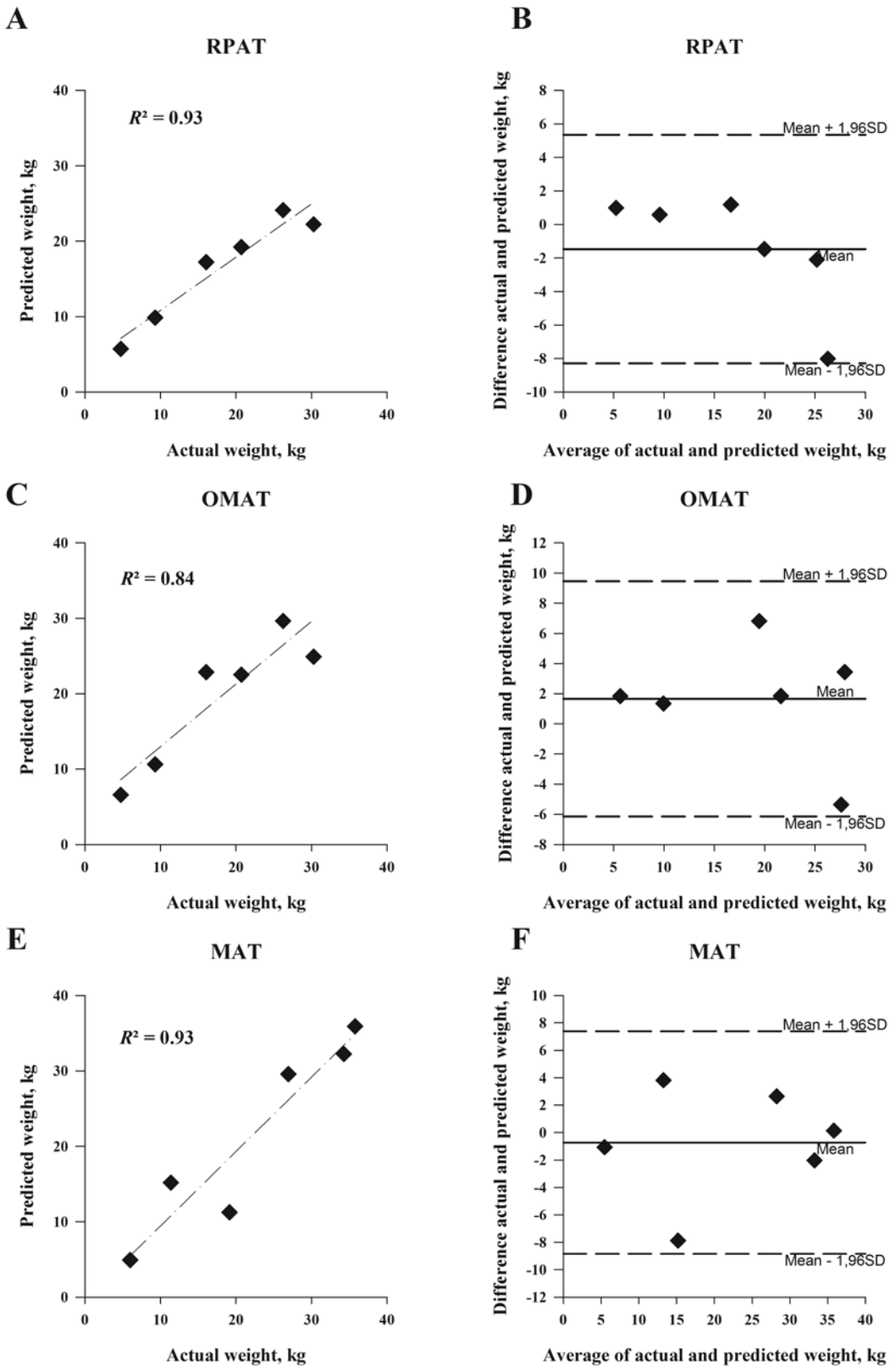

Figure 8. (A,C,E) Linear regression between the actual slaughter weight of an adipose tissue depot and its weight predicted by a multivariate linear regression model based on ultrasonographic measurements of fat layers in 6 test German Holsteins cows. (B, D, F) Bland–Altman plot of the difference between over the average of predicted and actual slaughter weights. RPAT = retroperitoneal adipose tissue; OMAT = omental adipose tissue; MAT = mesenterial adipose tissue

estimation of SCAT compared with the estimation of AAT and its components.

The slaughter weight of SCAT and AAT ranged from 5 to 43 kg and from 14 to 99 kg, respectively. The 3 components of AAT comprised about one-third each of the total amount. The multivariate regression analysis produced an RMSE of 3.4 kg for SCAT and 6.4 kg for AAT, which is in the range reported for physically separable internal body fat in beef cattle (Ribeiro and Tedeschi, 2012). The RMSE of RPAT, OMAT, and MAT varied between 1.7 and 3.2 kg. Therefore, the expected variance in ultrasonographically estimated fat depots attributable to inaccuracies of the presented technique is much smaller than the inter- and intraindividual biological variance of the different fat depots in dairy cows. Moreover, this study was limited to German Holstein cows older than 2 yr, and therefore, the findings may not apply to cattle of other breeds and those of a different age; fat distribution varies with age, breed, and production type in cattle (Pethick et al., 2004; Gotoh et al., 2009). However, formulae have been developed for the estimation of abdominal fat depots in different breeds of beef cattle (Ribeiro et al., 2008; Ribeiro and Tedeschi, 2012), suggesting that the type of cattle—beef or dairy—has a more profound effect on the amount and distribution of fat depots than the breed within a production type. The linear relationships between predicted and actual slaughter weights of fat depots in the 6 test cows (Fig. 8) were highly significant and had high coefficients of determination ($0.84 < R^2 < 0.98$). Also, the corresponding Bland–Altman plots showed, on average, only slight over- or underestimation of fat depots by means of developed regression equations.

Application of the regression models for assessment of different quantities of fat depots in transition cows revealed estimated amounts of fat in the different depots similar to depot quantities reported in an earlier study (von Soosten et al., 2011). von Soosten et al. (2011) used German Holstein heifers in their slaughter study, whereas in this study, pluriparous transition cows were investigated. This or differences in the slaughter protocol may explain the higher quantities in SCAT and MAT found in this study compared with results reported by von Soosten et al. (2011). In the application group, the expected dynamics of a quantitative increase during the dry period and a decrease after calving could be shown for the abdominal depots, whereas SCAT also decreased in fresh cows but did not significantly increase from −42 to 3 DIM. This again might point to time-dependent differences in accumulation and mobilization of fat stores in dairy cows during the transition period as postulated before (Rastani et al., 2001; Drackley et al., 2014; Pires et al., 2013).

However, the method presented in this study was developed in a relatively small number of cows and, therefore, is considered a proof of principle investigation. The accuracy of the formulae established for the calculation of various fat depots requires confirmation in future studies.

Conclusion

Ultrasonographic measurement of subcutaneous and retroperitoneal fat layers appears sufficiently precise for the clinical assessment of the amounts of SCAT, AAT, RPAT, OMAT, and MAT in dairy cows. If amounts of all adipose depots are to be assessed, 7 sonographic measurements in 6 locations are required. Because this is an in vivo measuring technique, it facilitates serial assessment of the adipose tissue distribution and dynamics over time during the production cycle of dairy cows. This method could be used to investigate the pathogenic role of visceral adipose tissue depots in LMS in dairy cows.

LITERATURE CITED

Drackley, J. K. 1999. Biology of dairy cows during the transition period: The final frontier? J. Dairy Sci. 82:2259–2273. doi:10.3168/jds.S0022-0302(99)75474-3

Drackley, J. K., R. L. Wallace, D. Graugnard, J. Vasquez, B. F. Richards, and J. J. Loor. 2014. Visceral adipose tissue mass in nonlactating dairy cows fed diets differing in energy density. J. Dairy Sci. 97:3420–3430. doi:10.3168/jds.2014-8014

Edmonson, A. J., I. J. Lean, L. D. Weaver, T. Farver, and G. Webster. 1989. A body condition scoring chart for Holstein dairy cows. J. Dairy Sci. 72:68–78. doi:10.3168/jds.S0022-0302(89)79081-0

Gotoh, T., E. Albrecht, F. Teuscher, K. Kawabata, K. Sakashita, H. Iwamoto, and J. Wegner. 2009. Differences in muscle and fat accretion in Japanese Black and European cattle. Meat Sci. 82:300–308. doi:10.1016/j.meatsci.2009.01.026

Härter, C. J., H. G. O. Silva, L. D. Lima, D. S. Castagnino, A. R. Rivera, O. B. Neto, R. A. Gomes, J. C. Canola, K. T. Resende, and I. A. M. A. Teixeira. 2014. Ultrasonographic measurements of kidney fat thickness and longissimus muscle area in predicting body composition of pregnant goats. Anim. Prod. Sci. 54:1481–1485.

Häussler, S. S., D. Germeroth, K. Friedauer, S. H. Akter, S. Danicke, and H. Sauerwein. 2013. Characterization of the dynamics of fat cell turnover in different bovine adipose tissue depots. Res. Vet. Sci. 95:1142–1150. doi:10.1016/j.rvsc.2013.07.004

Heinrichs, A. J., G. W. Rogers, and J. B. Cooper. 1992. Predicting body weight and wither height in Holstein heifers using body measurements. J. Dairy Sci. 75:3576–3581. doi:10.3168/jds.S0022-0302(92)78134-X

Hussein, H. A., A. Westphal, and R. Staufenbiel. 2013. Relationship between body condition score and ultrasound measurement of backfat thickness in multiparous Holstein dairy cows at different production phases. Aust. Vet. J. 91:185–189. doi:10.1111/avj.12033

Kabara, E., L. M. Sordillo, S. Holcombe, and G. A. Contreras. 2014. Adiponectin links adipose tissue function and monocyte inflammatory responses during bovine metabolic stress. Comp. Immunol. Microbiol. Infect. Dis. 37:49–58. doi:10.1016/j.cimid.2013.10.007

Kim, N., V. Amin, D. Wilson, G. Rouse, and S. Udpa. 1998. Ultrasound image texture analysis for characterizing intramuscular fat content of live beef cattle. Ultrason. Imaging 20:191–205. doi:10.1177/016173469802000304

Lancaster, P. A., G. E. Carstens, F. R. Ribeiro, M. E. Davis, J. G. Lyons, and T. H. Welsh Jr. 2008. Effects of divergent selection for serum insulin-like growth factor-I concentration on performance, feed efficiency, and ultrasound measures of carcass composition traits in Angus bulls and heifers. J. Anim. Sci. 86:2862–2871. doi:10.2527/jas.2008-1083

Lancaster, P. A., G. E. Carstens, F. R. Ribeiro, L. O. Tedeschi, and D. H. Crews. 2009. Characterization of feed efficiency traits and relationships with feeding behavior and ultrasound carcass traits in growing bulls. J. Anim. Sci. 87:1528–1539. doi:10.2527/jas.2008-1352

Locher, L., S. Häussler, L. Laubenthal, S. P. Singh, J. Winkler, A. Kinoshita, Á. Kenéz, J. Rehage, K. Huber, H. Sauerwein, and S. Dänicke. 2015. Effect of increasing body condition on key regulators of fat metabolism in subcutaneous adipose tissue depot and circulation of nonlactating dairy cows. J. Dairy Sci. 98:1057–1068. doi:10.3168/jds.2014-8710

Locher, L. F., N. Meyer, E.-M. Weber, J. Rehage, U. Meyer, S. Dänicke, and K. Huber. 2011. Hormone-sensitive lipase protein expression and extent of phosphorylation in subcutaneous and retroperitoneal adipose tissues in the periparturient dairy cow. J. Dairy Sci. 94:4514–4523. doi:10.3168/jds.2011-4145

Locher, L. F., J. Rehage, N. Khraim, U. Meyer, S. Dänicke, K. Hansen, and K. Huber. 2012. Lipolysis in early lactation is associated with an increase in phosphorylation of adenosine monophosphate-activated protein kinase (AMPK)a1 in adipose tissue of dairy cows. J. Dairy Sci. 95:2497–2504. doi:10.3168/jds.2011-4830

Peres, A. M., L. G. Dias, M. Joy, and A. Teixeira. 2010. Assessment of goat fat depots using ultrasound technology and multiple multivariate prediction models. J. Anim. Sci. 88:572–580. doi:10.2527/jas.2009-2195

Pethick, D. W., G. S. Harper, and V. H. Oddy. 2004. Growth, development and nutritional manipulation of marbling in cattle: A review. Aust. J. Exp. Agric. 44:705–715. doi:10.1071/EA02165

Pires, J. A., C. Delavaud, Y. Faulconnier, D. Pomies, and Y. Chilliard. 2013. Effects of body condition score at calving on indicators of fat and protein mobilization of periparturient Holstein-Friesian cows. J. Dairy Sci. 96:6423–6439. doi:10.3168/jds.2013-6801

Rastani, R. R., S. M. Andrew, S. A. Zinn, and C. J. Sniffen. 2001. Body composition and estimated tissue energy balance in Jersey and Holstein cows during early lactation. J. Dairy Sci. 84:1201–1209. doi:10.3168/jds.S0022-0302(01)74581-X

Ribeiro, F. R. B., and L. O. Tedeschi. 2012. Using real-time ultrasound and carcass measurements to estimate total internal fat in beef cattle over different breed types and managements. J. Anim. Sci. 90:3259–3265. doi:10.2527/jas.2011-4697

Ribeiro, F. R., L. O. Tedeschi, J. R. Stouffer, and G. E. Carstens. 2008. Technical note: A novel technique to assess internal body fat of cattle by using real-time ultrasound. J. Anim. Sci. 86:763–767. doi:10.2527/jas.2007-0560

Ripoll, G., M. Joy, J. Alvarez-Rodriguez, A. Sanz, and A. Teixeira. 2009. Estimation of light lamb carcass composition by in vivo real-time ultrasonography at four anatomical locations. J. Anim. Sci. 87:1455–1463. doi:10.2527/jas.2008-1285

Roche, J. R., N. C. Friggens, J. K. Kay, M. W. Fisher, K. J. Stafford, and D. P. Berry. 2009. Invited review: Body condition score and its association with dairy cow productivity, health, and welfare. J. Dairy Sci. 92:5769–5801. doi:10.3168/jds.2009-2431

Saremi, B., S. Winand, P. Friedrichs, A. J. Rehage, S. Dänicke, S. Häussler, G. Breves, M. Mielenz, and H. Sauerwein. 2014. Longitudinal profiling of the tissue-specific expression of genes related with insulin sensitivity in dairy cows during lactation focusing on different fat depots. PLoS ONE 9:e86211. doi:10.1371/journal.pone.0086211

Schröder, U. J., and R. Staufenbiel. 2006. Invited review: Methods to determine body fat reserves in the dairy cow with special regard to ultrasonographic measurement of backfat thickness. J. Dairy Sci. 89:1–14. doi:10.3168/jds.S0022-0302(06)72064-1

Shen, W., Z. Wang, M. Punyanita, J. Lei, A. Sinav, J. G. Kral, C. Imielinska, R. Ross, and S. B. Heymsfield. 2003. Adipose tissue quantification by imaging methods: A proposed classification. Obes. Res. 11:5–16. doi:10.1038/oby.2003.3

Staufenbiel, R. 1992. Energie- und Fettstoffwechsel des Rindes-Untersuchungskonzept und Messung der Rückenfettdicke. Mh. (In German.) Vet. Med. 47:467–474.

Staufenbiel, R. 1997. Konditionsbeurteilung von Milchkühen mit Hilfe der sonographischen Rückenfettdickemessung. (In German.) Prakt. Tierarzt Col. Vet. (In German.) 27:87–92.

Teixeira, A., M. Joy, and R. Delfa. 2008. In vivo estimation of goat carcass composition and body fat partition by real-time ultrasonography. J. Anim. Sci. 86:2369–2376. doi:10.2527/jas.2007-0367

Tienken, R., S. Kersten, J. Frahm, L. Hüther, U. Meyer, K. Huber, J. Rehage, and S. Dänicke. 2015a. Effects of prepartum dietary energy level and nicotinic acid supplementation on immunological, hematological and biochemical parameters of periparturient dairy cows differing in parity. Animals (Basel) 5:910–933.

Tienken, R., S. Kersten, J. Frahm, U. Meyer, L. Locher, J. Rehage, K. Huber, Á. Kenéz, H. Sauerwein, M. Mielenz, and S. Dänicke. 2015b. Effects of an energy-dense diet and nicotinic acid supplementation on production and metabolic variables of primiparous or multiparous cows in periparturient period. Arch Anim. Nutr. 69:319–339. doi:10.1080/1745039X.2015.1073002

von Soosten, D., U. Meyer, E. M. Weber, J. Rehage, G. Flachowsky, and S. Dänicke. 2011. Effect of *trans*-10, *cis*-12 conjugated linoleic acid on performance, adipose depot weights, and liver weight in early-lactation dairy cows. J. Dairy Sci. 94:2859–2870. doi:10.3168/jds.2010-3851

Wildman, E. E., G. M. Jones, P. E. Wagner, R. L. Boman, H. F. Troutt Jr., and T. N. Lesch. 1982. A dairy cow body condition scoring system and its relationship to selected production characteristics. J. Dairy Sci. 65:495–501. doi:10.3168/jds.S0022-0302(82)82223-6

Yang, X., and U. Smith. 2007. Adipose tissue distribution and risk of metabolic disease: Does thiazolidinedione-induced adipose tissue redistribution provide a clue to the answer? Diabetologia 50:1127–1139. doi:10.1007/s00125-007-0640-1